Cent. Eur. J. Phys. • 9(6) • 2011 • 1488-1492
DOI: 10.2478/s11534-011-0072-x

VERSITA

Central European Journal of **Physics**

First-principle calculations for electronic structure and bonding properties in layered $Na_2Ti_3O_7$

Research Article

Yongliang An[1], Zhonghua Li[2], Hongping Xiang[3], Yongjiang Huang[1], Jun Shen[1]*

1 *State Key Laboratory of Advanced Welding Production Technology, Harbin Institute of Technology, Harbin 150001, China*

2 *Key Laboratory of Micro-Systems and Micro-Structures Manufacturing, Ministry of Education, Harbin Institute of Technology, Harbin 150001, China*

3 *Department of Physics and Research Center OPTIMAS, University of Kaiserslautern, P.O. Box 3049, 67653 Kaiserslautern, Germany*

Received 20 March 2011; accepted 28 July 2011

Abstract: First-principles calculations of $Na_2Ti_3O_7$ have been carried out with density-functional theory (DFT) and ultrasoft pseudopotentials. The electronic structure and bonding properties in layered $Na_2Ti_3O_7$ have been studied through calculating band structure, density of states, electron density, electron density difference and Mulliken bond populations. The calculated results reveal that $Na_2Ti_3O_7$ is a semiconductor with an indirect gap and exhibits both ionic and covalent characters. The stability of the $(Ti_3O_7)^{2-}$ layers is attributed to the covalent bonding of strong interactions between O 2p and Ti 3d orbitals. Furthermore, the O atoms located in the innerlayers interact more strongly with the neighboring Ti atoms than those in the interlayer regions. The ion-exchange property is due to the ionic bonding between the Na^+ and $(Ti_3O_7)^{2-}$ layers, which can stabilize the interlayers of layered $Na_2Ti_3O_7$ structure.

PACS (2008): 71.15.Ap; 71.15.Mb; 71.22.+i; 77.84.Dy

Keywords: semiconductors • density functional theory • electronic structure • bonding property

1. Introduction

In recent years, sodium trititanate ($Na_2Ti_3O_7$) has received considerable attention due to its potential technological applications in various fields such as ion exchangers [1], photocatalysts [1–4], electrodes for secondary batteries [5], bioactive ceramics [6] and sensors [7]. Generally, it can be synthesized by solid state reactions [8] from TiO_2 and Na_2CO_3 or by sol-gel methods [9]. It is interesting that a large number of titanate nanostructures (i.e., nanotubes, nanowires, and nanobelts) have been widely obtained by a simple hydrothermal treatment of TiO_2 particles in NaOH solution [5, 10–14] since the first report on the successful synthesis of titanate nanotubes [15]. Though the detailed structure of these materials is under debate, it has been generally recognized that many sodium titanate nanomaterials crystallize as layered trititanate structures, suggested to be layers of $Na_2Ti_3O_7$. The $Na_2Ti_3O_7$ crys-

*E-mail: junshen@hit.edu.cn

tal belongs to a series of sodium titanates with chemical formula $Na_2Ti_nO_{2n+1}$ (n=3, 4, 5, 6) and is built up by three TiO_6 octahedra sharing two edges at one line, which are bonded together above and below by forming zigzag $(Ti_3O_7)^{2-}$ layers. The layers are held together by Na^+ ions which are situated at two different kinds of crystallographic sites [3]. Na^+ ions can be easily exchanged with different cations, such as Li^+, K^+, Fe^{3+}, Cu^{2+}, Zn^{2+}, Ni^{2+}, Co^{2+} and H^+ [16–22]. Due to the high-performance ion-exchange property of $Na_2Ti_3O_7$, it may be used for removal and recovery of heavy metal ions from industrial wastewaters [18], lithium-ion batteries and hydrogen storage materials [5, 16]. In contrast to extensive studies on the synthesis and modification of titanate nanostructures, very few theoretical studies were carried out [20, 23, 24]. Recently, Xu et al. [23] investigated the changes in the electronic property of Fe, Ni, and Na intercalation in $H_2Ti_3O_7$ and found that Fe and Ni atoms between the $(Ti_3O_7)^{2-}$ layers could lead to the improvement of photoabsorption in the visible light range, but Na^+ ions doping didn't change the band structure of $H_2Ti_3O_7$. Zhang and Wu [24] studied the thermodynamic properties of $Na_2Ti_3O_7$ under high temperatures and high pressures by ab initio study. Mori et al. [20] discussed the ionic substitutions in sodium titanate ($Na_{2-x}H_xTi_3O_7$) and pointed out that the ionic bonding tended to decrease after Na^+ ions were substituted by H^+ ions. Most theoretical studies were based on the effects of insertion of various ions into $Na_2Ti_3O_7$, however, the study on the electronic structure and structure stability has not been disclosed. In the present work, we study the electronic structure of $Na_2Ti_3O_7$ by first-principles calculations in order to reveal the relationship between the structure stability and chemical bonding properties. This work also provides some useful information for the studies of formation mechanisms of sodium titanate nanotubes.

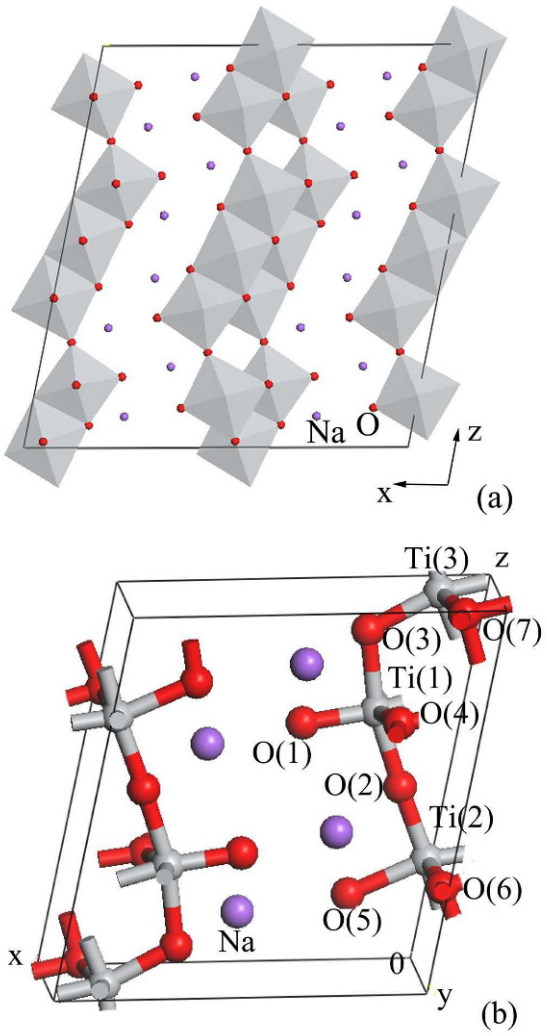

Figure 1. Crystal structures of $Na_2Ti_3O_7$ (a) Layered polyhedron structure on *xz* plane; (b) Unit cell. Red, gray and purple spheres indicate O, Ti and Na atoms, respectively. To make a clear description, Ti (1-3) and O (1-7) represent corresponding Ti and O atoms, respectively.

2. Computational method

First-principles calculations were performed with a plane-wave-based ultrasoft pseudopotential method within DFT, as implemented in Cambridge Serial Total Energy Package (CASTEP) [25]. The generalized gradient approximation with the Perdew-Bueke-Ernzerh scheme (GGA-PBE) approximation for the exchange-correlation functional was used [26]. The interactions between the electrons and the ion cores were represented by the Vanderbilt-type ultrasoft pseudopotentials [27]. The plane-wave cutoff energy was taken as 340 eV and the valence electron configurations were 3s23p63d24s2 for Ti atoms, 2s22p4 for O atoms, and 2s22p63s1 for Na atoms. The reciprocal-space integration over the Brillouin zone was carried out by using the Monkhorst-Pack scheme with $2 \times 5 \times 2$ k-sampling in the irreducible wedge. The lattice parameters and atomic positions were taken from Andersson and Wadsley's results [28], and relaxed during the structural optimization. The mechanical equilibrium was achieved through the conjugate gradient minimization of the total energy to a tolerance of 2.0×10-5 eV/atom, the forces to a tolerance of 0.05 eV/Å, and the atomic positions to a tolerance of 2×10-3 Å. The structure of $Na_2Ti_3O_7$ has a space group of P21/m. In this study, the $Na_2Ti_3O_7$ unit cell with 24 atoms was used as a structural model (Fig. 1).

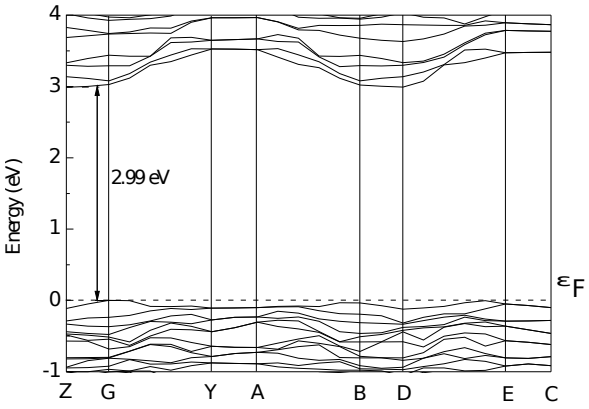

Figure 2. Calculated band structure of $Na_2Ti_3O_7$. The Fermi energy εF is taken as the zero of energy marked with dash lines.

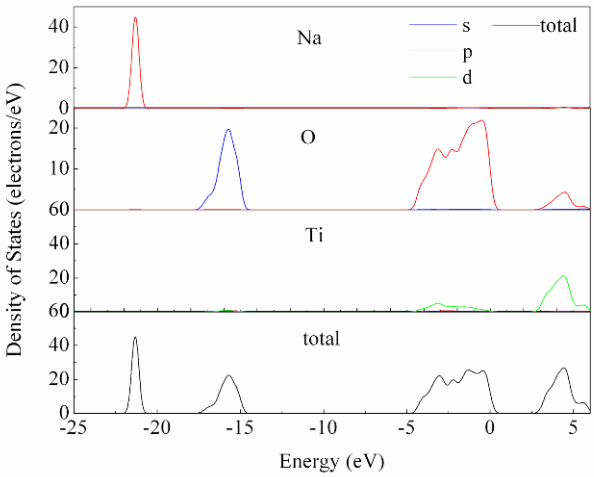

Figure 3. TDOS and PDOS of $Na_2Ti_3O_7$ in which s, p, d partial and total density of state of different atoms and unit cell are drawn in blue, red, green and black lines, respectively. The Fermi level is set as 0 eV.

3. Rsults and discussion

3.1. Band structure and density of states

After geometric optimization, the optimized equilibrium lattice constants ($a = 8.8340$ Å, $b = 3.8107$ Å, $c = 9.3597$ Å, and β=101.8489°) are close to the corresponding experimental values [28]. The deviations from the experimental values of a, b, c, and Îš are 3.07%, 0.18%, 2.5%, and 0.27%, respectively. These deviations are acceptable for DFT calculations so that all the calculations are performed based on these optimized values. The calculated band structure around the Fermi level is shown in Fig. 2. It can be seen that the top of the valence band and the bottom of the conduction band are located at $G(0, 0, 0)$ and $Z(0, 0, 0.5)$, respectively. $Na_2Ti_3O_7$ is a wide band gap semiconductor with the indirect gap of 2.99 eV, which is smaller than the experimental result (3.43 eV) [29] probably because of the fact that GGA often underestimates the band gap of materials [23]. In order to get into the details of the electronic structure of $Na_2Ti_3O_7$, the total density of states (TDOS) and partial density of states (PDOS) were plotted in Fig. 3. The bands in the energy range from -5 to 0 eV are predominantly occupied by O 2p orbitals with a small amount of Ti 3d orbitals. The quite similar pattern of the O 2p and Ti 3d orbitals indicates the strong hybridization was in between.

3.2. Electron density distribution

In Fig. 4, we present the electron density distribution on the (0, 4, 0) plane to illustrate the bonding structure. This map which labels three O atoms and one Ti atom (corresponding to O(1), O(2), O(3) and Ti(1) in the unit cell, Fig. 1b confirms that the chemical bonding of $Na_2Ti_3O_7$ are both ionic and covalent. The electrons of the Na atoms are only recognized as circles of contour lines between the $(Ti_3O_7)^{2-}$ layers and no local maxima of the electron distribution of the Na atoms can be seen. It may be due to the position of Na atoms which is far away from the $(Ti_3O_7)^{2-}$ layers. Therefore, the ionic characteristic between the Na atoms and $(Ti_3O_7)^{2-}$ layers is related to the position of Na atoms. In addition, the valence electron density distribution contour lines are shared by the Ti and O atoms. In other words, the electron density between the Ti and O atoms is not zero and the contour lines link them along octahedron diagonals. Therefore, such a bonding nature in the $Na_2Ti_3O_7$ indicates that the ionic bonding exists between the Na^+ and $(Ti_3O_7)^{2-}$ layers while the covalent bonding exists in the $(Ti_3O_7)^{2-}$ innerlayers. These results are consistent with the PDOS results above. The electron density distribution map can also indicate that the strong covalent bonding plays an important role in the stability of $Na_2Ti_3O_7$, depending on strong interactions between the O and Ti atoms. This is the main reason that $Na_2Ti_3O_7$ does not collapse and remains a layered structure in the process of ion-exchange even under strong alkali or acidic conditions. However, the ionic bonding can not be neglected, as it also contributes to stabilizing the interlayers. Once Na^+ ions were substituted by H^+ ions, the $(Ti_3O_7)^{2-}$ layers would tend to bend, roll, wrap and finally form nanotubes [30] because of the ionic bonding between $(Ti_3O_7)^{2-}$ layers being stronger than the hydro-

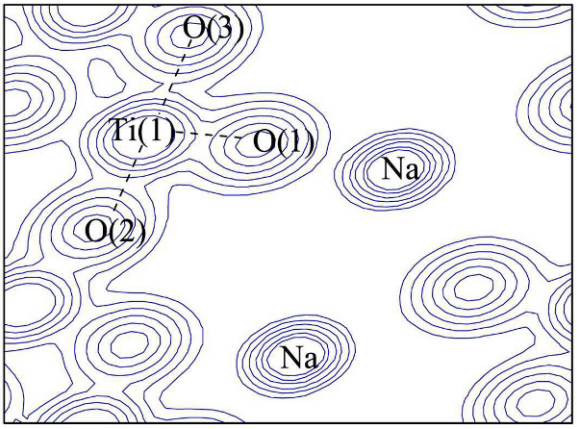

Figure 4. The electron density map on the (0, 4, 0) plane of $Na_2Ti_3O_7$. Contour lines are drawn at 3 electrons/Å^3 intervals.

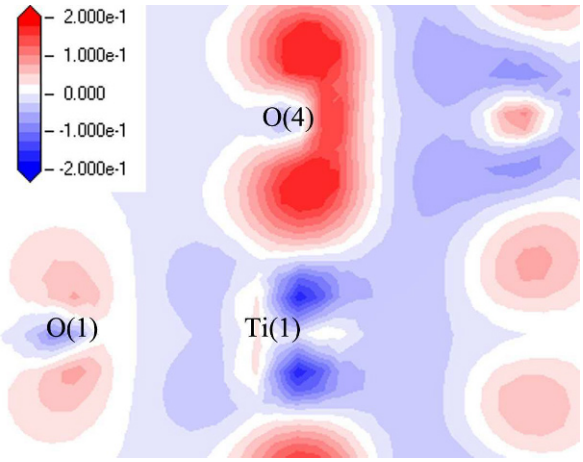

Figure 5. The electron density difference map of $Na_2Ti_3O_7$. The map is vertical to the [1 0 0] direction. The scale of this map (32 contour lines) is from -0.2 to 0.2 electrons /Å^3. Red or blue areas denote negative or positive electron density relative to the atom electron density respectively.

gen bonding due to the H^+ substitutions [20]. The role of the ionic bonding between the Na^+ layers and $(Ti_3O_7)^{2-}$ layers has also been found in titanate nanotubes [4, 18].

3.3. Electron density difference and Mulliken bond populations

The electron density difference is useful in the analysis of bonding characters of compounds. We calculate the electron density difference map (Fig. 5). The map is vertical to the [1 0 0] direction and through the central Ti atom (Ti(1)) of an octahedron and its two neighboring O atoms (O(1) and O(4)) in the unit cell. The negative and positive electron density distribution regions can be identified with bonding and anti-bonding electronic states, respectively. The charge transfer from Ti to O is conspicuous in the present case due to a large hybridization of the O 2p and Ti 3d orbitals. The electron density difference between Ti(1) and O(4) is shown to be much larger than that between Ti(1) and O(1) in the TiO6 octahedron, implying that Ti(1) forms a stronger bond with O(4) rather than O(1). The similar behavior of covalent character is found in other octahedra. This significant difference of bonding characters between the Ti and O atoms in one TiO6 octahedron results due not only to the distortion of the octahedron [28] but also to the different O positions in the layered structure. Here, it is important to note that there are two kinds of O positions: O(4), O(6) and O(7) which bond with Ti atoms along y axis are located in the innerlayers while other O atoms are located in the interlayers. Therefore, the O atoms located in the innerlayers have stronger covalent chemical bonding with neighboring Ti atoms than those in the interlayers. The

Table 1. Mulliken bond populations of partial Ti-O bonds.

Bond	Ti(1) -O(1)	Ti(1) -O(2)	Ti(1) -O(3)	Ti(1) -O(4)	Ti(2) -O(5)	Ti(2) -O(6)	Ti(3) -O(7)
Population	0.78	0.46	0.32	0.99	0.47	0.86	0.78

bonding behavior is also illustrated by the analysis of relevant Mulliken bond populations, as given in Table 1. A higher positive bond population indicates formation of a stronger covalent bond. The Mulliken bond population of the Ti(1)-O(4) bond (0.99) is larger than other Ti-O bonds (Ti(1)-O(2), 0.46; Ti(1)-O(3), 0.32; Ti(1)-O(1), 0.78) in the octahedron, therefore, the Ti(1)-O(4) bond shows a higher degree of covalency in the bond. Similar results can also be found in other Ti-O bonds, which is consistent with the electron density difference. The electron density difference and Mulliken bond populations results indicate that the different bonding characters of the Ti and O atoms rely on the different O positions: the O atoms located in the innerlayers have much stronger covalent chemical bonding with neighboring Ti than those in the interlayers, implying that it plays a key role in the stability of the innerlayers.

4. Conclusions

In this study, first-principles calculations using ultrasoft pseudopotential based on DFT were used to investigate the electronic structure and chemical bonding properties of

$Na_2Ti_3O_7$. Our results revealed that $Na_2Ti_3O_7$ is a semiconductor with an indirect gap and exhibits both ionic and covalent features in nature. The Na^+ ions located in the interlayers have ionic bonds with TiO_6 octahedra layers while the covalent bonds mainly contribute to the bonding between the Ti and O atoms by interactions between the O 2p and Ti 3d orbitals. Ti-O covalent bonds play a decisive role in stabilizing the $(Ti_3O_7)^{2-}$ layered structure. The O atoms located in the innerlayers have stronger covalent chemical bonding with neighboring Ti atoms than those in the interlayers. Our results will be useful for explaining the formation mechanism of sodium titanate nanotubes.

Acknowledgements

The authors gratefully acknowledge the support of Chinese National Hi-Tech Research & Development Program (863 Program, No. 2007AA03Z518), the National Natural Science Foundation of China under Grant No. 50802021, the Excellent Youth Foundation of Heilongjiang Province under Grant No. JC200806, and the Center of High Performance Computing of Harbin Institute of Technology.

References

[1] A. L. Sauvet, S. Baliteau, C. Lopez, P. Fabry, J. Solid State Chem. 177, 4508 (2004)
[2] J. Y. Tsai, J. H. Chao, C. H. Lin, J. Mol. Catal. A-Chem. 298, 115 (2009)
[3] N. Miyamoto, K. Kuroda, M. Ogawa, J. Mater. Chem. 14, 165 (2004)
[4] J. Suetake, A. Y. Nosaka, K. Hodouchi, H. Matsubara, Y. Nosaka, J. Phys. Chem. C 112, 18474 (2008)
[5] H. Zhang, X. P. Gao, G. R. Li, T. Y. Yan, H. Y. Zhu, Electrochim. Acta 53, 7061 (2008)
[6] I. Becker, I. Hofmann, F. A. Muller, J. Eur. Ceram. Soc. 27, 4547 (2007)
[7] Y Y. Zhang et al., Sensor Actuat. B-Chem 135, 317 (2008)
[8] J. Yang, D. Li, X. Wang, X. J. Yang, L. Lu, J. Mater. Sci. 38, 2907 (2003)
[9] S. Baliteau, A. L. Sauvet, C. Lopez, P. Fabry, Solid State Ionics 178, 1517 (2007)
[10] M. D. Wei, Z. M. Qi, M. Ichihara, I. Honma, H. S. Zhou, J. Nanosci. Nanotechno. 7, 1065 (2007)
[11] E. Morgado et al., Solid State Sci. 8, 888 (2006)
[12] W .P. Chen, X. Y. Guo, S. L. Zhang, Z. S. Jin, J. Nanopart. Res. 9, 1173 (2007)
[13] S. Sreekantan, L. C. Wei, J. Alloy Compd. 490, 436 (2010)
[14] Z. W. Tang, L. Q. Zhou, L. Yang, F. Wang, J. Alloy. Compd. 481, 704 (2009)
[15] T. Kasuga, M. Hiramatsu, A. Hoson, T. Sekino, K. Niihara, Langmuir 14, 3160 (1998)
[16] K. Chiba, N. Kijima, Y. Takahashi, Y. Idemoto, J. Akimoto, Solid State Ionics 178, 1725 (2008)
[17] L. M. Nunes, A. G. de Souza, R. F. de Farias, J. Alloy. Compd. 319, 94 (2001)
[18] X.M. Sun, Y. D. Li, Chem-Eur. J. 9, 2229 (2003)
[19] D. Maurya, P. Chand, J. Alloy. Compd. 459, 418 (2008)
[20] M. Mori, Y. Kumagai, K. Matsunaga, I. Tanaka, Phys. Rev. B 79, 144117 (2009)
[21] P. Umek et al., J. Phys. Chem. C 112, 15311 (2008)
[22] C. Díaz-Guerra, P. Umek, A. Gloter, J. Piqueras, J. Phys. Chem. C 114, 8192 (2010)
[23] X. G. Xu, X. Ding, Q. Chen, L. M. Peng, Phys. Rev. B 75, 035423 (2007)
[24] H. Zhang, H. Wu, Phys. Status Solidi B 245, 37 (2008)
[25] S. J. Clark et al., Z. Kristallogr. 220, 567 (2005)
[26] J. P. Perdew, K. Burke, M. Ernzerhof, Phys. Rev. Lett. 77, 3865 (1996)
[27] D. Vanderbilt, Phys. Rev. B 41, 7892 (1990)
[28] S. Andersson, A. D. Wadsley, Acta Crystallogr. 14, 1245 (1961)
[29] Z. Zhang et al., Dalton T. 39, 711 (2010)
[30] S. Zhang et al., Phys Rev. Lett. 91, 256103 (2003)